

# Journal of Parenteral and Enteral Nutrition

<http://pen.sagepub.com/>

---

## Probability-Based Compatibility Curves for Calcium and Phosphates in Parenteral Nutrition Formulations

Thomas Gonyon, Phillip W. Carter, Gerald Phillips, Heather Owen, Dipa Patel, Priyanka Kotha and John-Bruce D. Green

*JPEN J Parenter Enteral Nutr* 2014 38: 717 originally published online 26 July 2013

DOI: 10.1177/0148607113495415

The online version of this article can be found at:

<http://pen.sagepub.com/content/38/6/717>

---

Published by:



<http://www.sagepublications.com>

On behalf of:



American Society for Parenteral  
and Enteral Nutrition

[The American Society for Parenteral & Enteral Nutrition](#)

Additional services and information for *Journal of Parenteral and Enteral Nutrition* can be found at:

**Email Alerts:** <http://pen.sagepub.com/cgi/alerts>

**Subscriptions:** <http://pen.sagepub.com/subscriptions>

**Reprints:** <http://www.sagepub.com/journalsReprints.nav>

**Permissions:** <http://www.sagepub.com/journalsPermissions.nav>

>> [Version of Record](#) - Jul 16, 2014

[OnlineFirst Version of Record](#) - Jul 26, 2013

[What is This?](#)

# Probability-Based Compatibility Curves for Calcium and Phosphates in Parenteral Nutrition Formulations

Thomas Gonyon, BS; Phillip W. Carter, PhD; Gerald Phillips, MSc; Heather Owen, MSc; Dipa Patel, BS; Priyanka Kotha, MSc; and John-Bruce D. Green, PhD

Journal of Parenteral and Enteral Nutrition  
Volume 38 Number 6  
August 2014 717–727  
© 2013 American Society for Parenteral and Enteral Nutrition  
DOI: 10.1177/0148607113495415  
jpen.sagepub.com  
hosted at  
online.sagepub.com



## Abstract

**Background:** The information content of the calcium phosphate compatibility curves for adult parenteral nutrition (PN) solutions may benefit from a more sophisticated statistical treatment. Binary logistic regression analyses were evaluated as part of an alternate method for generating formulation compatibility curves. **Materials and Methods:** A commercial PN solution was challenged with a systematic array of calcium and phosphate concentrations. These formulations were then characterized for particulates by visual inspection, light obscuration, and filtration followed by optical microscopy. Logistic regression analyses of the data were compared with traditional treatments for generating compatibility curves. **Results:** Assay-dependent differences were observed in the compatibility curves and associated probability contours; the microscopic method of precipitate detection generated the most robust results. Calcium and phosphate compatibility data generated from small-volume glass containers reasonably predicted the observed compatibility of clinically relevant flexible containers. **Conclusions:** The published methods for creating calcium and phosphate compatibility curves via connecting the highest passing or lowest failing calcium concentrations should be augmented or replaced by probability contours of the entire experimental design to determine zones of formulation incompatibilities. We recommend researchers evaluate their data with logistic regression analysis to help build a more comprehensive probabilistic database of compatibility information. (*JPEN J Parenter Enteral Nutr.* 2014;38:717-727)

## Keywords

compatibility curves; particulate matter; experimental design; logistic regression; calcium phosphate; precipitation; parenteral nutrition

## Clinical Relevancy Statement

Pharmacists make use of published compatibility curves to make critical decisions concerning the dosing of calcium and phosphate concentrations in parenteral nutrition formulations. The researchers who generate these compatibility curves often-times perform extensive experimental designs, and usually only a few key data points at the edge of the compatibility zone are used to define the curve. The objective of the current study was to present the value of using logistic regression for generating information-rich compatibility curves. Logistic regression is a well-known form of analysis, which makes use of more of the experimental data and also generates information concerning the probability of failure at each calcium and phosphate pair. This extra information may provide the physicians and pharmacists with more valuable insight when weighing the clinical benefit vs the precipitation risk.

## Introduction

Pharmacists and clinicians rely on compatibility curves for compounding pharmaceutical formulations safely to meet their patients' therapeutic needs. There are multiple stability risk factors associated with parenteral nutrition (PN) admixtures.<sup>1-3</sup> One hazard specifically associated with calcium- and inorganic

phosphate-containing nutrition admixtures stems from the possible formation of calcium phosphate precipitates, which can lead to pulmonary emboli, respiratory distress, and even death.<sup>4-7</sup> Currently, calcium and phosphate compatibility curves specific to each parenteral formulation are found in texts and/or software packages.<sup>8</sup> Since these compatibility curves are compiled from various original sources representing diverse methodologies and compatibility criteria, a uniform interpretation of each compatibility curve is not always appropriate. Understanding these variations in compatibility curves

---

From Baxter Healthcare, Round Lake, Illinois.

Financial disclosure: This study was fully supported by Baxter Healthcare Corporation.

Supplementary material for this article is available on the *Journal of Parenteral and Enteral Nutrition* website at <http://pen.sagepub.com/supplemental>.

Received for publication March 1, 2013; accepted for publication June 4, 2013.

This article originally appeared online on July 26, 2013.

### Corresponding Author:

John-Bruce D. Green, PhD, Baxter Healthcare, Technology Resources, 25212 W. Illinois Route 120, Round Lake, IL 60073, USA.  
Email: [john\\_bruce\\_green@baxter.com](mailto:john_bruce_green@baxter.com)

and driving toward a clear, harmonized interpretation will further reduce patient risk during formulating and compounding activities.

Compatibility curve data are generally built by varying calcium and phosphate test compositions within a specific parenteral formulation and monitoring for evidence of precipitation. Although many factors are known to influence precipitation (pH, amino acid, calcium salt, phosphate type, temperature, and mixing),<sup>8-13</sup> the precipitation risk for individual test samples is evaluated using a pass-fail approach where compatible (pass) and incompatible (fail) zones are separated by a compatibility curve.

Table 1 enumerates references and highlights the diversified approaches to generating calcium phosphate compatibility curves. These approaches differ in their choice of storage conditions (time and temperature), test methods, and the rule used to draw the compatibility line. This work will not dwell on the storage conditions but instead will focus on the choice of test method and the manner of deriving the compatibility curves. As shown in Table 1, some researchers use the highest passing calcium concentration at each phosphate concentration, while others use the lowest failing calcium concentration at each phosphate concentration to generate their compatibility curves. These highest passing or lowest failing individual results are frequently connected by line segments to create the published compatibility curves. It is concerning that 2 separate compatibility curves can be generated for the same formulation data depending on the rules chosen. To add more complexity to this methodology, different precipitation assays are employed in making the pass-fail assignment. Visual inspection,<sup>9,11,14</sup> light obscuration particle-counting techniques,<sup>15-17</sup> and optical microscopy (membrane filters<sup>18-20</sup> or solutions<sup>21-25</sup>) are the 3 most common particle detection assays. The use of multiple detection methods is often employed to provide a more complete picture of calcium and phosphate compatibility as well.<sup>26-28</sup> Overall, the variations in rules and assays lead to an ambiguity that causes difficulty in the comparison and clear interpretation of published compatibility curves.

The approaches described above ultimately are attempting to provide the data required to construct an admixture-specific calcium-phosphate compatibility diagram and to clearly define zones where the risk of spontaneous particle formation is minimal. These particle nucleation events are stochastic in nature, and therefore generating statistically meaningful compatibility curves is challenging due to the large sample sizes needed. In fact, none of the studies referenced above were powered to provide precipitation probabilities as a function of admixture composition. More often, single-point to triplicate measurements are made per test condition over a broad array of calcium and phosphate concentrations. The most stressful test condition where no appreciable precipitate is detected typically represents a single point on the proposed compatibility curve (highest passing formalism). However, the probability of precipitation occurring if formulated on or just below the line

in a nominally "safe" region remains undefined in the current literature. Perhaps more problematic is the belief that there is a 0% chance of particle formation when formulating with just slightly lower calcium or phosphate concentrations relative to an established compatibility line.

This work describes the use of logistic regression applied to the pass-fail particle detection data to generate probabilistic compatibility curves. Although the logistic regression statistical tool is not new, its application to calcium-phosphate compatibility of PN formulations is unexplored. The added value to the analyses is the ease of defining the probability of failure (incompatibility) for each curve or each and every calcium and phosphate composition. As a case study, this work used a 5% amino acid/15% dextrose (5/15) code of Clinimix (Baxter, Deerfield, IL), which given the experimental design space was diluted by additives to a 4% amino acid/12% dextrose (4/12) formulation. In the comprehensive data set described below, the logistic regression curves are compared with the classically determined lowest failing and highest passing curves for the 3 most common methods for assessing precipitation (visual inspection, light obscuration, and filtration/microscopy). These resulting probabilistic compatibility curves may assist clinicians in the safe use of admixtures and could be incorporated into software tools designed to protect the patient.<sup>29</sup>

## Materials and Methods

### *PN Solutions*

The formulation considered for this work consisted of a premixed amino acid/dextrose PN solution (Clinimix 5/15 sulfite-free amino acid in dextrose solution, code 2B7709 or 2B7730; Baxter). This product is a sterile nonpyrogenic hypertonic solution in a flexible dual-chamber Clarity container (Baxter, Deerfield, IL) composed of a patented multilayer film<sup>30</sup> that contains a fluid-contacting layer of styrene-ethylene/butylene-styrene block copolymer. In this dual-chambered container, 1 chamber contains the amino acids and the other contains the dextrose, and after opening the seal between the chambers, the chambers are mixed thoroughly for use in the formulation below.

### *Formulation and Storage*

All test and control articles were prepared in a laminar flow hood. The order of addition was as follows: PN solution, sterile water (code 2B0304; Baxter), sodium chloride solution (23.4% 4 mEq/mL, code 2900-25 [American Regent, Shirley, NY] or 14.6% 2.5 mEq/mL, code 06657-73 [Hospira, Lake Forest, IL]), potassium chloride solution (2 mEq/mL, code 96520; APP, Schaumburg, IL), potassium phosphates (3 mmol/mL, code 2350-25; American Regent), and magnesium sulfate solution (4.06 mEq/mL, code 2610-25 [American Regent]; 0.325 mEq/mL, code 0409-6729-09 [Hospira]; or 4 mEq/mL, code 5491 [Sandoz, Boucherville, Canada]). All solutions were

**Table 1.** Published Methods for Generating Compatibility Curves.

Study	Product	Storage	Tests	Curve Definition	Category
Lenz and Mikrut, 1988 <sup>19</sup> Fitzgerald and MacKay, 1987 <sup>38</sup> Fitzgerald and MacKay, 1986 <sup>23</sup> Eggert et al, 1982 <sup>14</sup>	Aminosyn PF and/or TrophAmine	18 h/25°C; 30 min/37°C	Visual and microscopic	Plotting the concentration at which either visual or microscopic precipitation occurred	Lowest failing
Dunham et al, 1991 <sup>39</sup>	TrophAmine	23.5 h/RT; 30 min/37°C	Visual and Ca analysis	Line represents samples with visual cloudy appearance or visual crystals	Lowest Failing
Alexander and Arena, 1985 <sup>40</sup>	FreAmine III	24 h/RT	Visual only	Precipitation defined as test articles with calcium below 90% of initial value	Highest passing
Migaki et al, 2012 <sup>41</sup>	TrophAmine	23–24 h/37°C	Visual only	No curves generated. Table provided with maximum concentration without precipitation	Highest passing
Hoie and Narducci, 1996 <sup>42</sup>	TrophAmine	24 h/37°C	Visual and light obscuration	No curve generated. Trissel-generated curve based on highest concentration without precipitate	Highest passing
Zhang et al, 1999 <sup>28</sup>	Aminosyn II	48 h/23°C or 37°C	Visual and light obscuration	Highest concentration at which no precipitate formed	Highest passing
MacKay et al, 1996 <sup>25</sup>	HepatAmine NephrAmine	18 h/25°C; 30 min/37°C	Visual and microscopic	Plotting the highest calcium and phosphate that could be combined without observing precipitation	Highest passing
Poole et al, 1983 <sup>11</sup>	Aminosyn	30 h/25°C	Visual and microscopic	Area to right of the curve represents visual precipitation	Highest passing
Shatsky et al, 1995 <sup>20</sup>	TrophAmine	24 h/40°C	Visual and microscopic	No curve generated. Maximum amounts that were soluble presented in table used by Trissel to generate curve	Highest passing
Koorenhof and Timmer, 1992 <sup>24</sup>	Vamin	48 h/22°C and 37°C	Microscopic	Combinations on the curve gave no precipitation	Highest passing
Allwood, 1987 <sup>9</sup> MacKay et al, 2011 <sup>43</sup>	Vamin Glucose TrophAmine	24 or 48 h/37°C 30 min after compounding	Visual only Visual only	Not specified No curves generated	NA
Anonymous, 1995 <sup>44</sup>	Novamine Travasol	24 h/RT	Visual and microscopic	Not specified	
Rosen, 1999 <sup>45</sup>	Aminosyn II	24 h/RT; 30 min/37°C	Visual and microscopic	Not specified	
Anonymous, 2000 <sup>46,47</sup>	FreAmine III TrophAmine	24 h/ref; 24 h/25°C or 40°C	Visual and filtration	Not specified	

NA, information was not available; ref, refrigerated; RT, room temperature.

**Table 2.** Formulations for the 100-mL and 1-L Systems.

Component	Target Concentration	100-mL Actual Value or Range	1-L Actual Value or Range
Amino acid, %	4	4	4
Dextrose, %	12	12	12
Calcium, mEq/L	Varies	0–46.5	0–35.3
Phosphates, mmol/L	Varies	0–36	0–42
Sodium, mEq/L	150	148	148
Potassium, mEq/L	80	78.8–80.8	78.8–81.6
Magnesium, mEq/L	5	4.1	4.2
Acetate, mEq/L	34	33.6	33.6
Chloride, mEq/L	Varies	192–234	193–234

commercial solutions for injection. The samples were thoroughly mixed prior to addition of calcium gluconate (0.465 mEq/mL, code 3900-25; American Regent) and then thoroughly mixed once more. The addition of the electrolyte solutions diluted the amino acid concentration from an initial value of 5% to a range of values (4.1%–4.6%) depending on the exact electrolyte formulation. Formulas were prepared in 100 mL precleaned glass bottles with varying amounts of sterile water added to achieve a uniform final concentration of 4% amino acids and 12% dextrose in all containers, as seen in Table 2. The cleanliness of the bottles was ensured by exhaustive rinsing with filtered distilled water followed by testing with the light obscuration method to confirm minimal background particle counts (0 particles/mL greater than 2  $\mu$ m). All units were mixed by inverting the glass bottles 5 times prior to placing them in the environmentally controlled storage chambers. Test articles were first stored at  $25 \pm 2^\circ\text{C}$  for 24 hours, followed by a transfer to a second chamber set at  $40 \pm 2^\circ\text{C}$  for 24 hours of storage. The above conditions were intended to stress the test articles beyond both USP <797><sup>31</sup> (30 hours at  $20\text{--}25^\circ\text{C}$ ) and the specified current product insert instructions<sup>32</sup> of using promptly after mixing and any storage with additives refrigerated and limited to a brief period, less than 24 hours. After removal from the sample storage chamber and allowing them to reach ambient conditions, all samples were inverted prior to testing. Figure 1 shows the experimental design for this study with several different phosphate concentrations tested at several different calcium concentrations. In an effort to fully map the compatibility space, this design intentionally includes formulations too extreme for clinical applications. Some formulations are expected to precipitate calcium phosphate, whereas others are not. The entire range of the formulation space was prepared and tested, with calcium = (0, 4.7, 11.6, 18.6, 27.9, 37.2, and 46.5 mEq/L) and phosphates = (6, 12, 18, 24, 30, and 36 mmol/L). The formulation with 0 mEq/L of calcium and 18 mmol/L of phosphates functioned as the control sample, since it was not expected to precipitate calcium salts. Although the total phosphorous concentration was known from the addition of phosphates, the exact ratio of the different phosphate species was not measured, and although the pH of the experiments dictated that the ions were

predominantly the mono and divalent phosphate ions, for simplicity, we will hereafter refer to phosphates and use the symbol  $[P] = [\text{PO}_4^{3-}] + [\text{HPO}_4^{2-}] + [\text{H}_2\text{PO}_4^-] + [\text{H}_3\text{PO}_4]$ .

For samples with concentrations that demonstrated excessive visual precipitation (eg, 46.5 mEq/L calcium with 36 mmol/L phosphates), testing was limited to visual inspection. The quantity of precipitate in these cases was not quantified, but from experience, these samples would have formed a thick cake of precipitate had they been filtered for microscopy, or they may have plugged the light obscuration counter. In the second and third experiments, an additional phosphate series at  $[P] = 9$  mmol/L was added, and those formulations that generated excessive precipitation from the first experiment were not prepared in future experiments.

Using the results from the experiments with the 100-mL glass bottles, a series of formulations were created to systematically probe the breadth of the compatibility zone. These test formulations were prepared in activated 1-L dual-chambered containers to demonstrate the utility of the logistic regression

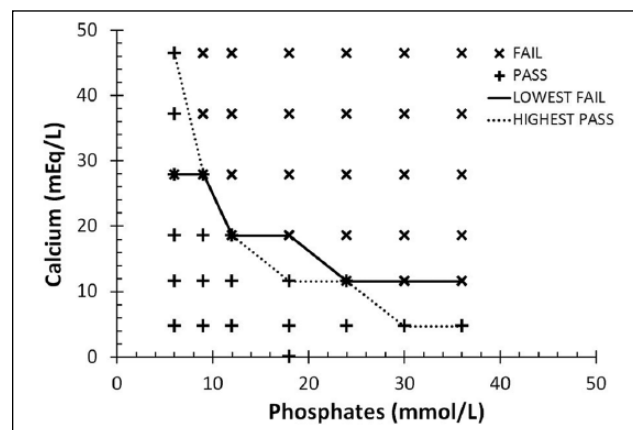


**Figure 1.** Compatibility curves are generated from triplicate microscopic measurements labeled as all pass (+), all fail (x), or at least 1 pass and 1 fail (\*). Connecting the highest calcium that passed at a given phosphate creates the highest pass curve (dotted line), and connecting the lowest calcium that failed creates the lowest fail curve (solid line).

contours for predicting the more clinically realistic containers. As with the 100-mL bottles, all 1-L test and control articles were prepared in a laminar flow hood and the order of addition was the same as previously with sterile water added to achieve a constant concentration of amino acids and dextrose in each container. The 1-L test and control articles were first stored at  $25 \pm 2^\circ\text{C}$  for 24 hours followed by a transfer to a second chamber set at  $40 \pm 2^\circ\text{C}$  for 24 hours' storage prior to performing the identical tests completed on the 100-mL containers.

### Visual Inspection

The visual inspection of the test solutions was completed by trained and prequalified analysts performing an untimed inspection of the entire test solutions for the presence or absence of visible particulates. The inspections were performed in a visual inspection booth incorporating both black and white backgrounds with overhead fluorescent lighting providing a minimum illumination of 500 foot-candles within the light box.<sup>33</sup> A positive visual result for precipitation was defined as the visual observation of any crystals, haziness, or cloudiness within the sample. In the event that the result was positive with a large amount of precipitate, no further particle testing was performed on that specific unit, and the microscopic and light obscuration tests were assumed to exceed the acceptance criteria for each test. For visually positive results where only a few crystals were observed or for samples with no visual crystals but where the haziness or cloudiness detected was barely perceptible, further particle testing with microscopic analysis and light obscuration particle counting was performed.

### Microscopic Analysis

A 50-mL aliquot from each unit that passed the visual test or had only a few crystals was filtered through a 0.8- $\mu\text{m}$  retention-rated cellulose ester filter membrane as described in USP <788><sup>34</sup> and USP <1788>.<sup>35</sup> The isolated particulate matter present on the test membranes was counted or characterized with a light microscope with lighting prescribed by USP <788>. However, only particulate matter that appeared crystalline was counted with a light microscope against the following limits: not more than (NMT) 6 particles/mL  $\geq 10 \mu\text{m}$  and NMT 1 particle/mL  $\geq 25 \mu\text{m}$ . These more stringent and somewhat arbitrary limits represent 50% of the USP limits for large volume injectable (LVI), which would normally correspond to NMT 12 particles/mL  $\geq 10 \mu\text{m}$  and NMT 3 particles/mL  $\geq 25 \mu\text{m}$ . This reduction is an effort to recognize that the USP <788> limits are intended for heterogeneous, randomly sourced extraneous particulate matter rather than the calcium phosphate crystals expected to be formed in this study.

### Light Obscuration Analysis

Particle size analysis and distribution of each formulation were determined using an AccuSizer Model 780 (Particle Sizing

Systems, Santa Barbara, CA) counter equipped with a syringe injection sampler using an LE 400 sensor in extinction mode previously calibrated with 2, 5, 10, 15, and 25  $\mu\text{m}$  of NIST traceable polystyrene latex spheres. Four sequential 4-mL aliquots from each test solution that passed the visual test or had only a few crystals present were evaluated with the AccuSizer particle counter determining the cumulative particle counts per milliliter greater than or equal to the following sizes: 1.5, 2.0, 5.0, 10.0, and 25.0  $\mu\text{m}$ . The results from the first 4-mL aliquot test from each sample were excluded from the average of the last 3 aliquots. The criterion for passing the light obscuration particle counts test was NMT 25 particles/mL cumulative counts for particles  $>10 \mu\text{m}$ , the same as the USP <788> light obscuration limits.

### pH Determination

The pH of each test solution was measured with an Orion PerpHecT LogR pH Meter, model 330 (Thermo Fisher Scientific, Boston, MA). The pH meter was calibrated prior to use, and a single pH measurement was performed for each solution.

### Logistic Regression Analysis

For the logistic regression analysis, each calcium and phosphate pairing was assigned a zero for a pass and a value of 1 for a failure according to each test method criterion. Logistic regression was used to fit the data from the 100-mL glass bottle experiments with a standard interaction model. The standard interaction model is as follows:  $\ln(p/(1-p)) = a_0 + a_1 [P] + a_2 [Ca] + a_{12} [P][Ca]$ , where [Ca] is the total calcium concentration, [P] is the total concentration of all phosphates,  $p$  is the probability of failing this specific test method, and  $a_0$ ,  $a_1$ ,  $a_2$ , and  $a_{12}$  are the logistic regression fitting constants. Table 2 provides the fitting coefficients corresponding to each of the 3 test assays, along with  $\chi^2$  goodness-of-fit values. The Hosmer and Lemeshow (HL)  $\chi^2$  goodness-of-fit test<sup>36</sup> was used to assess how well the 100-mL data were estimated by the logistic regression fits. To confirm the predictive value of the logistic regression, 10 calcium-phosphate pairs were run in triplicate for each test method using the 1-L dual-chambered containers. A  $\chi^2$  goodness-of-fit test was also used to assess how well the 100-mL-based logistic regression fits predict the 1-L plastic container probability of failure.

## Results

Figure 1 shows the experimental design space of the formulations and the results from the microscopic inspection of the formulation. The data corresponding to the figures can be found tabulated in the supplementary material. In all figures, the ( $\times$ ) symbols represent concentrations of calcium and phosphate where the formulation always exceeded (failed) the acceptance limit for that assay (microscopic, light obscuration,

or visual), and the (+) symbols represent those concentrations where the formulation always passed the assay. The (\*) symbols represent where there was at least 1 pass and 1 fail at the experimental condition probed.

Figure 1 also shows the 2 most common methods for generating the lines that separate the compatible and incompatible zones. One method, termed here *highest pass* and based on the literature referenced in Table 1, simply connects the highest passing calcium concentrations (highest “+” data point) at a given phosphate level using straight-line segments to “connect” the individual data points. Alternatively, the *lowest fail* method connects data points at the minimum calcium concentrations showing at least 1 failing data point at a fixed phosphate concentration. Simple regression analysis or other fitting functions may also be considered for generating compatibility curves based on goodness of fit, physical relevance, or a combination of both. Although the quality of the connect-the-dots approach and/or any fitting function will improve with an increasing number of replicates, the analysis will still be based on the data points represented by the highest passing or the lowest failing experimental conditions.

Figure 2 shows probability contours generated from the same data set shown in Figure 1 but using logistic regression analysis. As with any curve fitting, the choice of functional form is an important part of logistic regression. The standard interaction model was chosen because (1) it is a simple and direct model, and (2) the functional form allows for an inverse functional relationship between phosphate and calcium observed in the data. The logistic regression analysis uses all data points in generating the fitting coefficients, found in Table 3. These fitting coefficients are then used to generate the probability contours in Figure 2, which show the likelihood of exceeding the acceptance criteria for the microscopic test at various calcium and phosphate values. For example, a formulation prepared with calcium and phosphate values directly on the 50% line would have a 50% chance of exceeding the acceptance criteria and failing the microscopic test.

Figure 3 compares the 1-L data with the logistic regression predictive curves from Figure 2. The data that generated the regression curves have been removed so that the results from the 1-L dual-chambered container could be more easily visualized. The data from the 1-L samples are labeled 1–10

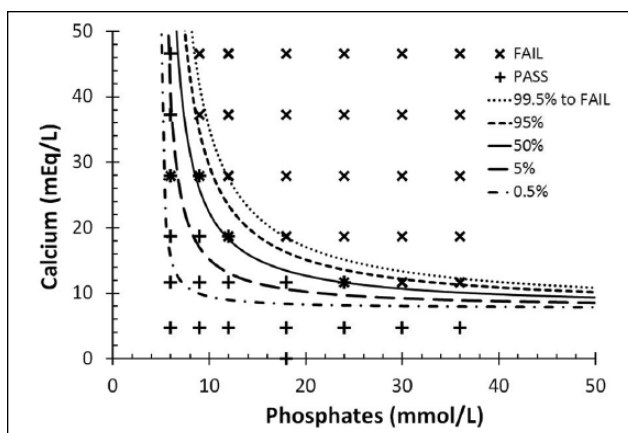


**Figure 2.** Compatibility curves generated from logistic regression. The contour curves correspond to specified probabilities of failing the microscopic assay (0.5%, 5%, 50%, 95%, and 99.5%).

correspond to the compositions listed in Table 4. Examination of Figures 2 and 3 shows that above the 95% probability of failure contour, there are no passing results for either the 100-mL or the 1-L containers. Near the 50% probability of failure contour, there are a roughly equal number of passes and failures whether considering the 100-mL or the 1-L containers. Finally, there was only 1 failure out of the ~50 measurements below the 5% probability of failure contour curve. Therefore, at a qualitative level, the microscopic results from the 1-L containers appear quite consistent with the results generated from the 100-mL containers.

The data from the light obscuration test method were analyzed in the same manner and generated logistic regression fitting constants, shown in Table 3, which in turn led to the probability of failure contours shown in Figure 4. As with the microscopic results in Figure 3, the light obscuration results in Figure 4 from the 1-L containers are comparable to the results from the 100-mL containers. However, unlike the microscopic assay, the light obscuration results contain more variability, as seen in the supplementary material, which effectively increases the width of the logistic regression transition region. This increased width can be directly perceived by comparing the

**Table 3.** Logistic Regression Fitting Coefficients.

Characteristic	$a_0$	$a_1$ , mmol/L	$a_2$ , mEq/L	$a_3$ , mmol·mEq/L <sup>2</sup>	HL Goodness of Fit		
					$\chi^2$	$df$	$\chi^2$ P Value
Microscopic	-3.13	-0.609	-0.380	0.0793	3.44	7	.84 <sup>a</sup>
Light obscuration	-5.32	-0.0327	-0.0629	0.0223	15.9	7	.03 <sup>b</sup>
Visual	-2.35	-0.116	-0.180	0.0223	17.0	8	.03 <sup>b</sup>

HL, Hosmer-Lemeshow.

<sup>a</sup>The model fits the data well.

<sup>b</sup>The model does not fit the data well at the .05 significance level.

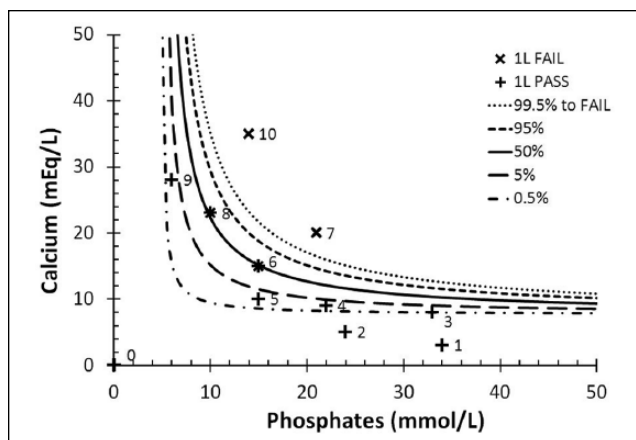


**Figure 3.** The 1-L compatibility data (microscopic assay) were mapped against the probability contours (microscopic assay) from the 100-mL glass bottle. The 1-L container data, measured in triplicate, are labeled 1–10 (Table 4), indicating pass (+), fail (×), or mixed results (\*).

size of the zone contained between adjacent contour lines such as 5% and 50% contours. The difference between 0.5% and 5% contours is also easy to distinguish when comparing Figures 3 and 4. Finally, Figure 5 shows the probability contours for the visual inspection assay, which were generated in an identical manner as the microscopic and light obscuration methods above. The visual assay seems to have the largest amount of variation, leading to even larger zones between neighboring contours.

In an effort to assess how well these logistic regression results fit the 100-mL data, the fitting results were tested with the HL  $\chi^2$  goodness-of-fit test. The output of this test is included along with the fitting constants in Table 3. Because the null

hypothesis for this test was that the model fits the data well, a high  $P$  value suggests a good fit. Using the logistic regression fitting constants derived from the 100-mL data, it is possible to compute the probability for failure for calcium and phosphate values in the 10 different 1-L formulations. Table 4 provides a comparison of the 100-mL predicted probability of failure with the observed probability of failure for the 1-L containers, along with the  $\chi^2$  test statistic, degrees of freedom, and  $P$  value for each test method. Similarly, in this case, a high  $P$  value suggests a good agreement between the data sets, and therefore the  $P$  values indicate that the current 100-mL–based logistic regression models predicted the 1-L data well for each of the 3 test methods. Because the 1-L data were performed in triplicate, the probabilities of failure are quantized as 0%, 33%, 67%, and 100%, and given the coarse nature of these bins, it is not surprising that the predicted and the observed numeric values are not identical.

### Discussion

Figure 1 represents the commonplace practice in the literature of simply connecting the highest pass (dotted lines) or the lowest fail (solid lines) and equating these “curves” to the compatibility curve. Frequently, the number of replicates that were performed is not disclosed in the literature, but equally problematic is that it is contingent on the practitioners to track down these differences in assignment of “lowest fail” or “highest pass” from the original publications. Thus, the practitioner may interpret all compatibility curves with the same confidence and meaning when differences may exist. For example in this work, the lowest fail method of determining calcium-phosphate compatibility in Figure 1 is quite comparable to the 50% pass-fail probability contour of Figure 2, in which both

**Table 4.** Logistic Regression Predictability for 1-L Containers.

ID	Phosphates, mmol/L	Calcium, mEq/L	Microscopy, %		Light Obscuration, %		Visual, %	
			Predicted	Observed	Predicted	Observed	Predicted	Observed
1	34	3	0	0	1	0	1	0
2	24	5	0	0	2	0	3	0
3	33	8	0	0	27	0	15	33
4	22	9	1	0	10	0	11	0
5	15	10	2	0	4	0	7	0
6	15	15	47	33	15	33	15	100
7	21	20	100	100	89	33	73	100
8	10	23	57	33	12	0	8	0
9	6	28	2	0	3	0	1	0
10	14	35	100	100	95	67	66	100
$\chi^2$			0.23		1.26		5.9	
$df$			10		10		10	
$P$ value			1.00 <sup>a</sup>		1.00 <sup>a</sup>		.82 <sup>a</sup>	

<sup>a</sup>The current model fits the data well.



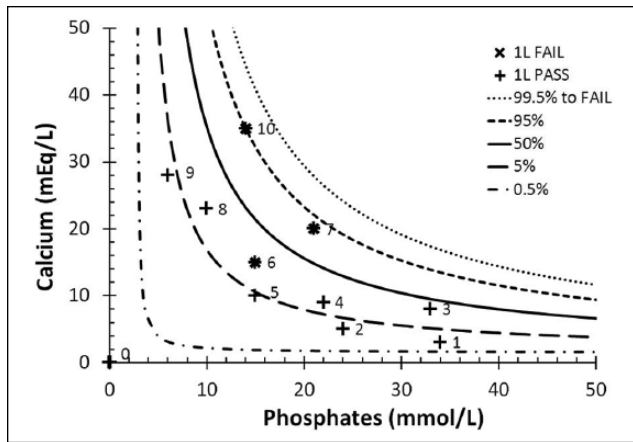


**Figure 4.** The 1-L compatibility data (light obscuration assay) were mapped against the probability contours (light obscuration assay) from the 100-mL glass bottle. The 1-L container data, measured in triplicate, are labeled 1–10 (Table 4), indicating pass (+), fail (x), or mixed results (\*).

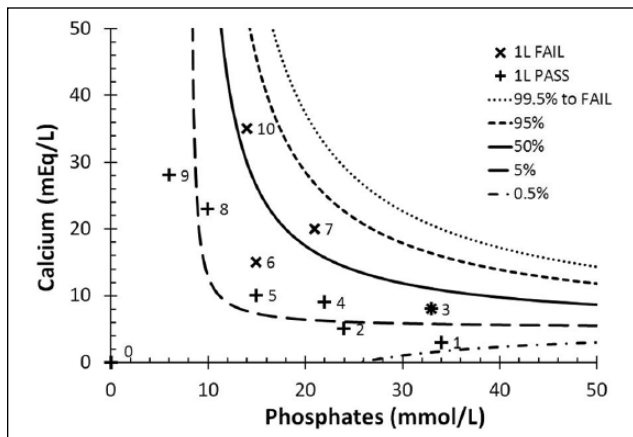


**Figure 5.** The 1-L compatibility data (visual inspection assay) were mapped against the probability contours (visual inspection assay) from the 100-mL glass bottle. The 1-L container data, measured in triplicate, are labeled 1–10 (Table 4), indicating pass (+), fail (x), or mixed results (\*).

were based on an identical microscopic data set. A formulation prepared with calcium and phosphate concentrations directly on the 50% line would have a 50:50 chance of exceeding the acceptance criteria for the microscopic test. Although this may be an unexpected result, the example illustrates the value of more standardized acquisition, analyses, and presentation of compatibility data.

Due to differing operating principles and limits of detection, it is not surprising that the different assays can generate unique compatibility curves. The visual inspection assay is by definition insensitive to subvisible particles that would precede the larger, visible precipitates via nucleation and growth mechanisms of particle formation. Although light obscuration can

be used to detect subvisible particles, the method does not unambiguously discriminate between environmental and precipitation sourced particulate. In addition, the visual and light obscuration methods cannot be applied to opaque solutions such as concentrated emulsions. These methods would require substantial dilution to render the emulsion transparent, and such a dilution may reduce the precipitate counts below detection.

Based on the data collected here, the 50% contour shifts to the right (higher phosphate concentrations) as the method is changed from microscopic to light obscuration and then to visual. As an example, the formulation with 9 mmol/L phosphate and 37 mEq/L calcium has ~99% probability for failing the microscopic assay while also having ~50% probability of failing the light obscuration assay and only ~5% probability for failing the visual inspection assay. Thus, the microscopic assay has the highest sensitivity to particle formation, and in this context, it is the most conservative approach in building compatibility curves.

In addition, the logistic regression fits shown in Figures 3–5 highlight the apparent band or range of probability from the 0.5%–99.5% probability of failing the assay, the assay failure zone. The width of this zone allows one to assess the sensitivity of the formulation to failing the specific assay as a function of the formulation variables. For the formulations measured in this study, as the calcium and phosphate concentrations are varied, the visible assay failure zone is very broad, the light obscuration zone is tighter, and the microscopic assay has the narrowest zone. Overall, this is attributed to the fact that, for this specific set of experiments, the data from the microscopic method have the least variation in pass-fail data for a given solution condition. From this point of view, although more labor intensive, the microscopic assay produced better results when compared with the light obscuration–based single-particle optical sensing and visual assays.

Although small glass containers are convenient for compatibility analysis primarily due to scale, accessibility, and ease of use, they do not reflect the container types or volume scales encountered in clinical applications. As an important final step in assessing risk, compatibility curves generated with model systems were compared with data from more clinically relevant containers. Inspection of Figures 3–5 shows that the 100-mL glass bottle–generated probability contours seem to be in good agreement with sample data from the 1-L containers. Table 4 further illustrates this agreement by comparing the predicted probability (from 100-mL glass containers) with the observed probability based on triplicate measures of the 1-L samples. For data point 7 (21 mmol/L phosphate, 20 mEq/L calcium), the visual inspection showed a failure probability of 100%, where it was predicted to be only 15%, and thus represents a significant deviation. The microscopic assay seemed the most reliable evidenced by matched probabilities at (1) the 100% failure predictions, (2) 0% failures, and (3) intermediate probabilities for data points 6 and 8. In the limited context of

this example and for the microscopic assay, switching container types and solution volumes appears to have no significant impact on calcium and phosphate compatibility. The  $P$  values in Table 4 indicate that the current 100-mL–based logistic regression models fit the 1-L data well for each assay. Researchers interested in extending the relevance of the compatibility curves for a given parenteral formulation could increase the variables from calcium and phosphate to include other variables such as shipping, storage, and reformulation conditions with a smaller design of experiments, as was implemented for container type here.

There are a few additional technical details to consider when evaluating the logistic regression–based probability data. The first is the choice of the function used with the logistic regression. In this work, a standard interaction model was chosen, in which the [Ca], [P], and an interaction product, [Ca][P], were treated as separate variables. More complicated cubic models, which included higher order terms such as [Ca][P]<sup>2</sup>, were also examined using stepwise algorithms. In this case, the more complex models did not produce better fits to the data, based on the HL  $\chi^2$  goodness-of-fit test. The specific functional form of the standard interaction model places certain restrictions on the functional form of the probability contours. For example, it is not possible for this basic interaction model to generate a peak in the contour plots; however, a detailed explanation of the nuances related to the exact functional forms and their impact on the results is outside the scope of this article. The output from logistic regression analysis of the data is not always in the functional form familiar to users, as illustrated in Figure 5 for the 0.5% probability contour for the visual inspection test method. Although implementation of the logistic regression–based probability contours will require an increased level of sophistication, it is expected to lead to higher quality of information.

The choice of experimental design remains critical to efficient generation of quality compatibility information. This work used a grid-based experimental design, which was acceptable for this study; however, moving forward, perhaps there are better designs. There is limited value in testing numerous formulations that are deep in the 0% or 100% probability of failing zones. Therefore, a coarse grid design could be used to gain insight into a formulation zone where there are intermediate probabilities of failure, and then a systematic formulation design could be targeted throughout and around this zone. Although replicates are always valuable, in a resource-limited experimental design, the use of logistic regression in this way would de-emphasize the need for replicate measurements at identical formulations to establish “highest passing” criteria. Incrementally unique formulations are easily incorporated in analytical treatments to provide a finer resolution between contours produced by logistic regression. Minimizing gaps in the key formulation space will enable the full utility of logistic regression. This experimental approach can be further streamlined with the use of modern automated electron microscopy

systems that are capable of automatically measuring and identifying (elementally) thousands of particles per filter membrane in the range of minutes to hours. This could enable rapid screening of formulation space for precipitation-based incompatibilities.

Although this article focused on precipitation-based compatibility, some of the ideas can be readily extended to other incompatibilities and even drug interactions. Given the binary output (pass or fail) with regard to USP methods, logistic regression seems appropriate for determining the fitting, and while the detailed functional form may be varied to obtain the best fit to the data, the resulting probability of failure contours should be more useful to pharmacists. In general, the compounding space can always be divided into “compatible” and “incompatible” zones. By selecting an assay with appropriate acceptance criteria and by making measurements at key points in this formulation space, logistic regression analysis can be used to generate the probability for the formulation failing the predefined acceptance criteria.

This work used a premixed formula as the case study for generating the probabilistic compatibility information. Although many pharmacies make use of concentrated amino acid formulations that are compounded on demand, the premixed formulas are limited to lower total concentrations. These premixed formulations (eg, Clinimix 5/15) are intended for central vein infusion and may not be appropriate for all applications. When augmented with lipids, these formulations supply the needed amounts of protein, fat, energy, and water for most mildly to moderately ill patients. Similarly, the electrolyte conditions were chosen not as the typical or standard values but instead to reflect extreme electrolyte levels, which, although potentially outside safety limits, are sometimes administered to patients who may require higher amounts of electrolytes due to excessive losses or increased metabolic demands.<sup>37</sup>

## Conclusion

Experimental design and statistical analysis using logistic regression have been used to generate improved calcium-phosphate compatibility curves that include probability contours. Probability contours for a PN formulation were generated using a matrix of calcium- and phosphate-containing solutions. The probability contours generated for 100-mL test solutions in glass showed that at lower phosphate concentrations, the microscopic test method generated the most robust and conservative compatibility curves. The light obscuration method was less conservative, and the visual method of particle detection was the least conservative of the 3 assays with the largest zones between selected contour lines. The results demonstrate that the uncertainties associated with a single compatibility curve for each formulation can be replaced by contour plots indicating the probability of failure/incompatibility. The application of logistic regression analysis offers superior information

quality when compared with either the connect-the-dots approach or the linear regression of highest passing or lowest failing formulations. The probabilistic contours define the calcium and phosphate region of compatibility in a quantitative manner that is potentially more readily accessible, understandable, and accurate. We recommend the retrospective evaluation of compatibility data with logistic regression analysis and that future compatibility curves plan for logistic regression analysis in experimental designs to help build more comprehensive probabilistic databases. This will enable a shift in the communication of calcium phosphate precipitation information away from single curves with no probability information to a probability-based assessment of each proposed formulation. With time, infrastructure development, and training, this higher quality probabilistic information would be integrated into software for use in a clinical environment while remaining backward compatible for products where probabilistic data do not exist. Presently, based on the available data contained here, we propose using the 5% microscopic curve (5% chance of exceeding the microscopic criteria) as the most appropriate probability-based compatibility curve to be applied for patients.

### Acknowledgments

We thank Christine Holly, MSc, for verification of various data tables, as well as Laura Gripman, MSc, RD, and Tom Westercamp, MSc, RPh, for their discussions and guidance.

### References

- Pertkiewicz M, Cosslett A, Mühlebach S et al. Basics in clinical nutrition: stability of parenteral nutrition admixtures. *e-SPEN*. 2009;4:e117-e119.
- Wormleighton CV, Catling TB. Stability issues in home parenteral nutrition. *Clin Nutr*. 1998;17(5):199-203.
- Bouchoud L, Sadeghipour F, Klingmuller M, et al. Long-term physicochemical stability of standard parenteral nutrition for neonates. *Clin Nutr*. 2010;29(6):808-812.
- Knowles JB, Cusson G, Smith M, et al. Pulmonary deposition of calcium phosphate crystals as a complication of home total parenteral nutrition. *JPEN J Parenter Enteral Nutr*. 1989;13(2):209-213.
- Lumpkin MM. Safety alert: hazards of precipitation associated with parenteral nutrition. *Am J Hosp Pharm*. 1994;51(11):1427-1428.
- McKinnon BT. FDA safety alert: hazards of precipitation associated with parenteral nutrition. *Nutr Clin Pract*. 1996;11(2):59-65.
- Shay DK, Fann LM, Jarvis WR. Respiratory distress and sudden death associated with receipt of a peripheral parenteral nutrition admixture. *Infect Control Hosp Epidemiol*. 1997;18(12):814-817.
- Trissel LA. *Calcium and Phosphate Compatibility in Parenteral Nutrition*. Houston, TX: TriPharma Communications; 2001.
- Allwood MC. The compatibility of calcium phosphate in paediatric TPN infusions. *J Clin Pharm Ther*. 1987;12(5):293-301.
- Allwood MC, Kearney MC. Compatibility and stability of additives in parenteral nutrition admixtures. *Nutrition*. 1998;14(9):697-706.
- Poole RL, Rupp CA, Kerner JA Jr. Calcium and phosphorus in neonatal parenteral nutrition solutions. *JPEN J Parenter Enteral Nutr*. 1983;7(4):358-360.
- Driscoll DF, Newton DW, Bistrrian BR. Precipitation of calcium phosphate from parenteral nutrient fluids. *Am J Hosp Pharm*. 1994;51(22):2834-2836.
- Driscoll DF. Stability and compatibility assessment techniques for total parenteral nutrition admixtures: setting the bar according to pharmaceutical standards. *Curr Opin Clin Nutr Metab Care*. 2005;8(3):297-303.
- Eggert LD, Rusho WJ, MacKay MW, et al. Calcium and phosphorus compatibility in parenteral nutrition solutions for neonates. *Am J Hosp Pharm*. 1982;39(1):49-53.
- Parikh MJ, Dumas G, Silvestri A, et al. Physical compatibility of neonatal total parenteral nutrient admixtures containing organic calcium and inorganic phosphate salts. *Am J Health Syst Pharm*. 2005;62(11):1177-1183.
- Joy J, Silvestri AP, Franke R, et al. Calcium and phosphate compatibility in low-osmolarity parenteral nutrition admixtures intended for peripheral vein administration. *JPEN J Parenter Enteral Nutr*. 2010;34(1):46-54.
- Bouchoud L, Fonzo-Christe C, Sadeghipour F, et al. Maximizing calcium and phosphate content in neonatal parenteral nutrition solutions using organic calcium and phosphate salts. *JPEN J Parenter Enteral Nutr*. 2010;34(5):542-545.
- Li LC, Chang HC, Sampogna T. Prediction of calcium phosphate precipitation in 3-in-1 total nutrient admixtures: an apparent solubility product approach. *Pharm Sci*. 1996;2(4):165-168.
- Lenz GT, Mikrut BA. Calcium and phosphate solubility in neonatal parenteral nutrient solutions containing Aminosyn-PF or TrophAmine. *Am J Hosp Pharm*. 1988;45(11):2367-2371.
- Shatsky F, McFreely EJ, Takahashi D. A table for estimating calcium and phosphorus compatibility in parenteral nutrition formulas that contain TrophAmine plus cysteine. *Hosp Pharm*. 1995;30(8):690-692.
- Wong JC, McDougal AR, Tofan M, et al. Doubling calcium and phosphate concentrations in neonatal parenteral nutrition solutions using monobasic potassium phosphate. *J Am Coll Nutr*. 2006;25(1):70-77.
- Ribeiro DdO, Lobo BW, Volpato NM, et al. Influence of the calcium concentration in the presence of organic phosphorus on the physicochemical compatibility and stability of all-in-one admixtures for neonatal use. *Nutr J*. 2009;8(51):1-13.
- Fitzgerald KA, MacKay MW. Calcium and phosphate solubility in neonatal parenteral nutrient solutions containing TrophAmine. *Am J Hosp Pharm*. 1986;43(1):88-93.
- Koorenhof MJC, Timmer JG. Stability of total parenteral nutrition supplied as 'all-in-one' for children with chemotherapy-linked hyperhydration. *Pharm Weekbl Sci*. 1992;14(2):50-54.
- MacKay MW, Fitzgerald KA, Jackson D. The solubility of calcium and phosphate in two specialty amino acid solutions. *JPEN J Parenter Enteral Nutr*. 1996;20(1):63-66.
- Ronchera-Oms CL, Jimenez NV, Peidro J. Stability of parenteral nutrition admixtures containing organic phosphates. *Clin Nutr*. 1995;14(6):373-380.
- Driss Chaieb S, Sfar S, Chaumeil JC. Calcium and phosphates compatibilities in parenteral nutrition admixtures. *Tunis Med*. 2006;84(11):677-682.
- Zhang Y, Xu Q, Trissel LA, et al. Physical compatibility of calcium acetate and potassium phosphates in parenteral nutrition solutions containing Aminosyn II. *Int J Pharm Compound*. 1999;3(5):415-420.
- Canada T, Albrecht J. Parenteral calcium gluconate supplementation: efficacious or potentially disastrous? *J Am Coll Nutr*. 1998;17(4):401-403.
- Becker M, Masterson M, Desbrosses F, inventors; Baxter International Inc, assignee. Containers and methods for storing and admixing medical solutions. US patent 6,319,243. 2001.
- Chapter <797>: Pharmaceutical compounding—sterile preparations. In: *United States Pharmacopeia* [35th rev] and the *National Formulary* [30th ed]. Rockville, MD: United Book Press; 2011:350-387.
- CLINIMIX sulfite-free (amino acid in dextrose) injections [product insert]. rev. 07-19-57-358. Deerfield, IL: Baxter Healthcare Corporation; 2010.
- Barber TA. Visual inspection. In: *Pharmaceutical Particulate Matter: Analysis and Control*. Buffalo Grove, IL: Interpharm Press; 1993:25.

34. Chapter <788>: Particulate matter in injections. In: *United States Pharmacopeia* [35th rev] and the *National Formulary* [30th ed]. Rockville, MD: United Book Press; 2011:5157-5159.
35. Chapter <1788>: Methods for the determination of particulate matter in injections and ophthalmic solutions. In: *United States Pharmacopeia* [35th rev] and the *National Formulary* [30th ed]. Rockville, MD: United Book Press; 2011:945-954.
36. Hosmer DW, Stanley L. *Applied Logistic Regression*. 2nd ed. New York, NY: John Wiley; 2000.
37. Mirtallo J, Johnson D, Kumpf V, et al. Safe practices for parenteral nutrition. *JPEN J Parenter Enteral Nutr*. 2004;28(6):S39-S70.
38. Fitzgerald KA, MacKay MW. Calcium and phosphate solubility in neonatal parenteral nutrient solutions containing Aminosyn PF. *Am J Hosp Pharm* 1987;44(6):1396-1400.
39. Dunham B, Marcuard S, Khazanie PG, et al. The solubility of calcium and phosphorus in neonatal total parenteral nutrition solutions. *JPEN J Parenter Enteral Nutr*. 1991;15(6):608-611.
40. Alexander SR, Arena R. Predicting calcium phosphate precipitation in premature infant parenteral nutrition solutions. *Hosp Pharm*. 1985;20:656-658.
41. Migaki EA, Melhart BJ, Dewar CJ, et al. Calcium chloride and sodium phosphate in neonatal parenteral nutrition containing TrophAmine precipitation studies and aluminum content. *JPEN J Parenter Enteral Nutr*. 2012;36(4):470-475.
42. Hoie EB, Narducci WA. Laser particle analysis of calcium phosphate precipitate in neonatal TPN admixtures. *J Pediatr Pharm Pract*. 1996;1(3):163-167.
43. MacKay M, Jackson D, Eggert L, et al. Practice-based validation of calcium and phosphorus solubility limits for pediatric parenteral nutrition solutions. *Nutr Clin Pract*. 2011;26(6):708-713.
44. Anonymous. Novamine and Travasol calcium phosphate solubility curves, from Baxter Healthcare Corp. 1995. In: Trissel LA, ed. *Calcium and Phosphate Compatibility in Parenteral Nutrition*. Houston, TX: TriPharma Corporation; 2001:82.
45. Rosen PD. Personal communication, 1999. In: Trissel LA, ed. *Calcium and Phosphate Compatibility in Parenteral Nutrition*. Houston, TX: TriPharma Corporation; 2001:14.
46. Anonymous. Maximum calcium and phosphorous concentrations for FreAmine III TPN and PPN solutions, from B. Braun Medical Inc. 2000. In: Trissel LA, ed. *Calcium and Phosphate Compatibility in Parenteral Nutrition*. Houston, TX: TriPharma Corporation; 2001:46.
47. Anonymous. Calcium/phosphate compatibility in TPN solutions containing Trophamine (6% and 10% amino acids injections), from B. Braun Medical Inc. 2000. In: Trissel LA, ed. *Calcium and Phosphate Compatibility in Parenteral Nutrition*. Houston, TX: TriPharma Corporation; 2001:98.